THE ASTROPHYSICAL JOURNAL, 475:L107–L110, 1997 February 1

VARIATION OF MOLECULAR LINE RATIOS AND CLOUD PROPERTIES IN THE ARP 299 GALAXY MERGER

S. AALTO
Division of Physics, Mathematics, and Astronomy, Caltech 105-24, Pasadena CA 91125; sab@caltech.edu

SIMON J. E. RADFORD
National Radio Astronomy Observatory, 949 North Cherry Avenue, Tucson, AZ 85721-0665; sradford@nrao.edu

AND

N. Z. SCOVILLE AND A. I. SARGENT
Division of Physics, Mathematics, and Astronomy, Caltech 105-24, Pasadena CA 91125; nzs@caltech.edu, afs@caltech.edu
Received 7 August 1996; accepted 1996 November 13

ABSTRACT

High-resolution observations of ^{12}CO (2.″3), ^{13}CO (3.″9), and HCN (5.″4) $J = 1–0$ in the galaxy merger Arp 299 (IC 694 and NGC 3690) show that the line ratios vary dramatically across the system. The ^{12}CO/^{13}CO ratio is unusually large, 60 ± 15, at the IC 694 nucleus, where ^{12}CO emission is very strong, and much smaller, 10 ± 3, in the southern extended disk of that galaxy. Elsewhere, the ^{12}CO/^{13}CO line ratio is 5–20, typical of spiral galaxies. The line ratio variation in the overlap between the two galaxies is smaller, ranging from 10 ± 3 in the east to 20 ± 4 in the west.

The ^{12}CO/HCN line ratio also varies across Arp 299, although to a lesser degree. HCN emission is bright toward each galaxy nucleus and in the extranuclear region of active star formation; it was not detected in the IC 694 disk or the eastern part of the overlap region, leading to lower limits of 25 and 20, respectively. By contrast, at the nuclei of IC 694 and NGC 3690 the ratios are 9 ± 1 and 14 ± 3, respectively. In the western part of the overlap region it is 11 ± 3.

The large ^{12}CO/^{13}CO 1–0 intensity ratio at the nucleus of IC 694 can primarily be attributed to a low-to-moderate optical depth ($\tau \lesssim 1$) in the ^{12}CO 1–0 line. These data support the hypothesis that unusually high ^{12}CO/^{13}CO line ratios (>20) are associated with extremely compact molecular distributions in the nuclei of merging galaxies. Relative to ^{12}CO, ^{13}CO 1–0 is brightest in quiescent regions of low ^{12}CO surface brightness and weakest in starburst regions and the galactic nuclei. A medium consisting of dense ($n = 10^4$–10^5 cm^{-3}) and warm ($T_k > 50$ K) gas will reproduce the extreme line ratios observed in the nucleus of IC 694, where the area filling factor must be at least 20%.

Subject headings: galaxies: evolution — galaxies: individual (Arp 299) — galaxies: ISM — galaxies: starburst — radio lines: galaxies — radio lines: ISM

1. INTRODUCTION

The inner kiloparsecs of starburst and interacting galaxies harbor stunning amounts of molecular gas, 10^9–10^{10} $M_\odot$ (e.g., Scoville et al. 1991; Bryant & Scoville 1996). In these environments, molecular clouds are subject to intense radiation fields, supernovae explosions, winds from newborn hot stars, strong tidal forces, and gas surface densities several orders of magnitude higher than in the Milky Way disk. These are also extremely active star formation sites. Knowledge of the physical conditions and structure of molecular gas in interacting systems is essential in understanding the starburst activity and its role in galaxy evolution.

Arp 299 is an IR-luminous ($L_{\rm IR} \approx 8 \times 10^{11}$ $L_\odot$) merger system of two galaxies, IC 694 and NGC 3690. Strong ^{12}CO emission has been detected from the nuclei of IC 694 and NGC 3690 and from the interface between the two galaxies (Solomon & Sage 1988; Casoli et al. 1989; Sargent et al. 1987; Sargent & Scoville 1991). The two nuclei, as well as the western overlap region, currently harbor intense star formation activity (see Gehrz, Sramek, & Weedman 1983; Baan & Haschick 1990). Furthermore, the nucleus of IC 694 is a flat-spectrum radio source and may be an active galactic nucleus (AGN) (Gehrz et al. 1983).

Lower resolution (single-dish) observations reveal an unusually large ^{12}CO/^{13}CO 1–0 line intensity ratio, $\gtrsim$20 in Arp 299 (Aalto et al. 1991; Casoli, Dupraz, & Combes 1992). These observations left it unclear whether this is due to weak ^{13}CO in the whole system or to a varying ^{12}CO/^{13}CO 1–0 line ratio. Observations at 20″ and 11″ resolution by Casoli et al. (1992) suggest little variation in the ^{12}CO/^{13}CO 1–0 line ratio and none in the ^{12}CO/^{13}CO 2–1 line ratio. In contrast, Aalto et al. (1995) note substantial variations at 28″ resolution in the ^{12}CO/^{13}CO 2–1 ratio: the ratio is about 17 in IC 694, close to 9 in NGC 3690, and about 7 in the interface region between the two disks. Solomon et al. (1992) detected bright HCN emission in 28″ maps of Arp 299. They measured ^{12}CO/HCN ratios of 11 in IC 694 and 13 in the interface region.

2. OBSERVATIONS AND RESULTS

Aperture synthesis ^{12}CO, ^{13}CO, and HCN 1–0 mapping of Arp 299 was carried out with the Owens Valley Radio Observatory (OVRO) millimeter array between 1995 March and 1996 February. SIS receivers on the six 10.4 m telescopes provided typical system temperatures (SSB) of 600 K, 450 K, and 350 K for ^{12}CO, ^{13}CO, and HCN. Quasars 1150+497 and 0917+449 were used for phase calibration, and Uranus and Neptune for absolute flux calibration. The synthesized beams are 2.″5 × 2.″2 for ^{12}CO (uniform weighting), 4.″3 × 3.″6 for ^{13}CO (natural weighting), and 5.″6 × 5.″3 for HCN (natural

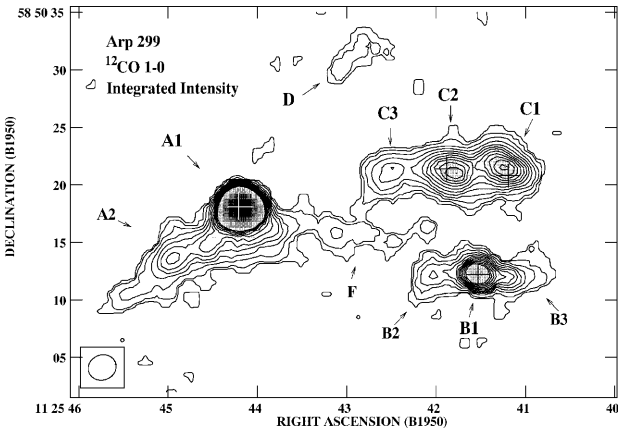

FIG. 1*a*

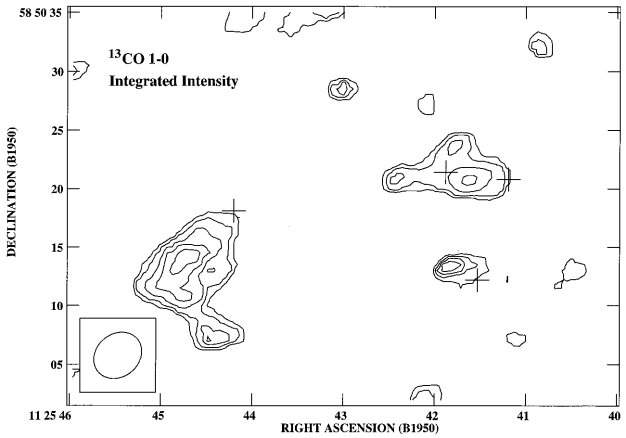

FIG. 1*b*

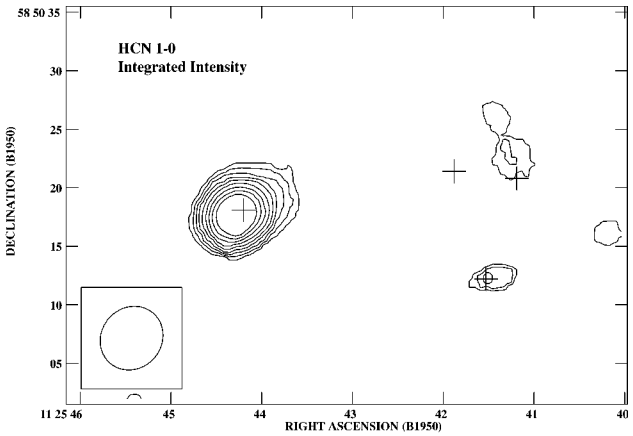

FIG. 1*c*

FIG. 1.—(*a*)^{12}CO 1–0 moment map (2800–3400 km s^{-1}). Contour levels are 0.9, 1.8, 3.6, 5.4, 7.2, 9, 10.8, 12.6, 14.4, 16.2, and 18 Jy beam^{-1} km s^{-1} . Gray-scale levels range from 5 to 75 Jy beam^{-1} km s^{-1} . The peak flux is 97 Jy beam^{-1} km s^{-1} on the nucleus of IC 694. Crosses mark the 6 cm radio continuum positions (Gehrz et al. 1983). (*b*) The ^{13}CO 1–0 moment map. Contour levels are 0.4, 0.8, 1.2, 1.6, and 2.0 Jy beam^{-1} km s^{-1} . The peak flux is 2.3 Jy beam^{-1} km s^{-1} on the disk of IC 694. (*c*) HCN 1–0 moment map. Contour levels are 0.6, 1.2, 1.8, 2.4, 3.0, 3.6, 4.2, 4.8, and 5.4 Jy beam^{-1} km s^{-1} . The peak flux is 7.1 Jy beam^{-1} km s^{-1} at the nucleus of IC 694.

weighting). At 2.6 mm wavelength with 2″.3 resolution, a brightness temperature of 1 K corresponds to 57 mJy beam^{-1}. The digital correlator, centered at $V_{\rm LSR}$ = 3100 km s^{-1}, provided a total velocity coverage of 1123 km s^{-1} for ^{12}CO, 1175 km s^{-1} for ^{13}CO, and 1407 km s^{-1} for HCN. Data were binned to 4 MHz resolution, corresponding to 10 km s^{-1} for ^{12}CO and ^{13}CO and 13 km s^{-1} for HCN. At 110 GHz an unresolved continuum source of 17 ± 2 mJy was detected in the center of IC 694. Continuum emission was also detected in NGC 3690 (5 ± 2 mJy) and the overlap region (9 ± 2 mJy). We subtracted this continuum emission from the line emission before maps were made.

The main structures found by Sargent & Scoville (1991) with the three-telescope array are recovered in our new ^{12}CO map (Fig. 1*a*), but our increased *uv* coverage enables improved deconvolution. Lower surface brightness emission (A2), possibly a molecular disk or bar, extends 10″–15″ southeast of the IC 694 nucleus (A1), coincident with the remnant optical disk. The center of NGC 3690 (B1) is also surrounded by weak, extended emission (B2 and B3) with a somewhat S-shaped morphology. Where the two galaxies overlap, three distinctive clumps (C1, C2, and C3) can now be discerned. Weaker, extended emission is also recovered better in our new ^{12}CO map, and clumpy structures can be distinguished at the center of the map (F). These structures appear to connect the major components A, B, and C. In addition, there is a clump (D) north of the main features with systemic velocity ≈3280 km s^{-1}, which is beyond the bandwidth of the earlier OVRO data.

Bright 6 cm radio continuum peaks at the nuclei of IC 694 and NGC 3690 (Gehrz et al. 1983; Condon et al. 1991) coincide with the ^{12}CO peaks to within the estimated positional uncertainty (0″.5). There is also reasonable positional agreement between the two brightest ^{12}CO clumps in the overlap region (C) and two additional 6 cm radio continuum peaks: C1 and the western radio continuum peak are also coincident within 0″.5, although the discrepancy between C2 and the eastern radio continuum peak is somewhat larger, $\Delta\alpha$ = 0″.8. Weaker radio continuum emission at 18 cm and 6 cm is spatially coincident with the extended ^{12}CO emission in regions A2, B2, B3, and F (Baan & Haschick 1990; Gehrz et al. 1983).

The velocity field image (Fig. 2 [Pl. L13]) reveals a monotonic shift from the blueshifted emission from A2 in IC 694 to redshifted emission from the overlap region C and from region D. Velocity gradients within C and D are small. The velocity field of NGC 3690 is complicated by a double-peaked emission structure of B2, and both B2 and B3 appear blueshifted relative to the center, B1.

TABLE 1

ARP 299: SOURCE PROPERTIES

REGION	SIZE[a] (arcsec)	^{12}CO 1–0 INTENSITY Peak (Jy km s^{-1} beam^{-1})	Integrated (Jy km s^{-1})	$\Delta V_{\rm FWHM}$ (km s^{-1})	$\frac{^{12}\rm CO\ 1–0^b}{^{13}\rm CO\ 1–0}$	$\frac{^{12}\rm CO\ 1–0^b}{\rm HCN\ 1–0}$
IC 694: nucleus (A1)	$\lesssim$1.4	97	122	350	60 ± 15	9 ± 1
IC 694: disk (A2)	17 × 6[c]	12	120	65	10 ± 3	>25 (3 σ)
NGC 3690: nucleus (B1)	$\lesssim$1.5	29	36	260	⋯	⋯
NGC 3690: total	⋯	⋯	53	⋯	13 ± 2	14 ± 3
Overlap east (C3)	3.4 × 2.2	9	15	60	10 ± 3	>20 (3 σ)
Overlap west (C2)	4.3 × 2.1	20	40	80	⋯	⋯
Overlap west (C1)	3.9 × 2.0	21	47	60	20 ± 4	11 ± 3
Region D	⋯	⋯	4	80	5 ± 3	>10
Region F	⋯	⋯	11	40–80	⋯	⋯

[a] FWHM from two-dimensional Gaussian fits using the AIPS task IMFIT.

[b] All ratios are in terms of integrated brightness temperatures. Uncertainties include thermal noise only. The ^{12}CO map was smoothed to the resolution of the ^{13}CO or HCN map before line ratios were constructed.

[c] An estimate of the size of the southeast disk of IC 694—no Gaussian fit possible.

The nuclei of both IC 694 (A1) and NGC 3690 (B1) remain unresolved by our 2.″2 synthesized beam. A two-dimensional Gaussian fit to the nuclear emission of IC 694 and NGC 3690 yields upper limits to the source diameters of 1.″4 and 1.″5, corresponding to radii of 140 and 150 pc, respectively (for D = 42 Mpc). This implies a lower limit of 18 K to the ^{12}CO brightness temperature in the IC 694 nucleus, and therefore, the cloud filling factor is quite high in the inner 200 pc. Even if the intrinsic brightness temperature is as high as 100 K, the surface filling factor of clouds is still almost 20%. The three features in the overlap region are resolved, with sizes of 792 × 322 pc (C1), 876 × 428 pc (C2), and 684 × 456 pc (C3). Derived properties for all designated regions are presented in Table 1.

The total molecular mass of Arp 299, estimated from $M(\rm H_2) = 1.2 \times 10^4 S\Delta v D^2\, M_\odot$ (D is the distance in Mpc, $S\Delta v$ is the integrated ^{12}CO 1–0 line flux in Jy K km s^{-1}), is 7.5 × 10^9 $M_\odot$, 87% of the value estimated by Solomon & Sage (1988) from their single-dish map. This formula corresponds to $N(\rm H_2)/I(^{12}CO) = 3 \times 10^{20}$ cm^{-2} (K km s^{-1})$^{-1}$ (Sargent & Scoville 1991), a standard Galactic ^{12}CO luminosity to $\rm H_2$ mass ratio. The conversion factor may vary, however, across Arp 299, since the line ratios indicate different cloud properties.

The most striking feature of the ^{13}CO 1–0 map (Fig. 1*b*) is the *absence of strong emission at the nucleus of IC 694 (A1)*. Emission *is* detected in the A2 region of IC 694, in the overlap region C, and in NGC 3690. Unlike Casoli et al. (1992), we find significant variation in the ^{12}CO/^{13}CO 1–0 line ratio across Arp 299. From the very high value of 60 ± 15 at the IC 694 nucleus (A1), the ratio drops to 10 ± 3 in the A2 region. The global ratio for NGC 3690 is 13 ± 2, but there is an indication that the ratio is higher in the nucleus, B1, than in B2 or B3. The ratios for the east (C3) and west (C1) overlap region are 11 ± 3 and 20 ± 4, respectively. The spatial correlation between the ^{13}CO emission and radio continuum emission peaks is also poor.

As for ^{12}CO, the HCN map (Fig. 1*c*) is dominated by a peak at the center of IC 694 (A1), where the ^{12}CO/HCN line ratio is 9 ± 1. Emission is also detected at the nucleus of NGC 3690, where the ratio is 14 ± 3, and in the western (C1) overlap region, where ^{12}CO/HCN = 11 ± 3. There is very little HCN in regions A2 and C3. The HCN and ^{13}CO line emission peaks appear anticorrelated.

3. THE MOLECULAR LINE RATIOS

As a system, Arp 299 is not deficient in ^{13}CO. In all regions but the core of IC 694, we observe ^{12}CO/^{13}CO line ratios typical of star-forming regions in other galaxies (e.g., Aalto et al. 1995, 1991; Young & Sanders 1986; Rickard & Blitz 1985). Relative to ^{12}CO, ^{13}CO 1–0 is brightest in quiescent regions of low ^{12}CO surface brightness, and weak in starburst regions and galactic nuclei. In contrast, HCN 1–0, like ^{12}CO, is bright in the two galaxy centers and in regions of active star formation. These line ratio variations are most likely caused by differences in line excitation. Our results support the suggestion (Aalto et al. 1995) that *unusually* high (i.e., >20) ^{12}CO/^{13}CO 1–0 line ratios tend to be associated with extremely compact molecular distributions centered on the nuclei of merging galaxies and are primarily due to a small or moderate optical depth, $\tau \lesssim 1$, in the ^{12}CO 1–0 line. High ambient pressures, strong tidal forces, and ongoing starburst or AGN activity lead to substantial changes in cloud structure and physical conditions. Bryant (1996) also finds that HCN 1–0 is bright in regions of high ^{12}CO surface brightness in merging galaxies.

3.1. *IC 694*

The line ratio variation from the IC 694 disk, where ^{12}CO/^{13}CO = 10 and ^{12}CO/HCN $\gtrsim$ 25, to its nucleus, where the corresponding values are 60 and 9, reflects a dramatic change in cloud properties.

The bright HCN line accompanied by relatively weak ^{13}CO emission (HCN/^{13}CO = 7 ± 2) implies a population of unusually dense and warm clouds. The HCN 1–0 strength implies densities $n \gtrsim 10^4$ cm^{-3} if the HCN excitation is dominated by collisions with $\rm H_2$. It is also likely that the density is $\lesssim 10^5$, so that most of the HCN population will remain in the lower levels and $\tau_{10} > 1$. At these densities, the ^{12}CO and ^{13}CO 1–0 transitions are thermalized. If the kinetic temperature is also high, the lower levels may become significantly depopulated, effectively reducing the optical depth of the 1–0 line. Then the ^{13}CO 2–1/1–0 line ratio should be greater than 1. Comparing the single-dish ^{13}CO 2–1 flux (Aalto et al. 1995) with our ^{13}CO 1–0 flux from the nucleus of IC 694, we estimate that ^{13}CO 2–1/1–0 $\gtrsim$ 2, implying that the gas temperature is high, greater than 50 K. Although the single-dish beam was large, 28″, the bulk ($\gtrsim$65%) of the ^{12}CO 2–1 emission within the beam originates in the nucleus of IC 694 (A1).

Since the lower transitions of ^{12}CO and ^{13}CO appear ther-

malized, LTE can be assumed to estimate the ^{12}CO column density, $N(^{12}\mathrm{CO})$. We find it unlikely that the $^{12}\mathrm{CO}/^{13}\mathrm{CO}$ abundance ratio is extremely high (§ 3.3). Therefore, a high $^{12}\mathrm{CO}/^{13}\mathrm{CO}$ 1–0 line ratio indicates a low-to-moderate optical depth ($\tau \lesssim 1$) in the $^{1\,2}$CO 1–0 line. The high intrinsic ^{12}CO 1–0 brightness temperature makes $\tau \ll 1$ unlikely, and we therefore assume that $\tau_{10}(^{12}\mathrm{CO}) \approx 1$. The optical depth of the 1–0 transition can be expressed as $\tau_{10}(^{12}\mathrm{CO}) \approx 3.9 \times 10^{-15} N(^{12}\mathrm{CO})(1 - e^{-5.53/T_{\mathrm{ex}}})/T_{\mathrm{ex}}\Delta V$. For a temperature $T_{\mathrm{ex}} = 100$ K, line width $\Delta V = 5$ km s^{-1}, and $\tau_{10} = 1$, the ^{12}CO column density $N(^{12}\mathrm{CO}) = 2 \times 10^{18}$ cm^{-2} (per cloud), and the resulting brightness temperature $T_B(^{12}\mathrm{CO}) \approx 60$ K. For a density of $n = 10^4$ cm^{-3} and a ^{12}CO abundance, $[^{12}\mathrm{CO}/\mathrm{H_2}] = 5 \times 10^{-5}$, the cloud radius $r = N(^{12}\mathrm{CO})/2x(^{12}\mathrm{CO})n(\mathrm{H_2}) = 0.7$ pc—not unlike cores or clumps within giant molecular clouds in the Galaxy. At this gas density, HCN is not thermalized, so T_{ex}(HCN) for the 1–0 line will be significantly lower than that for ^{12}CO. If the abundance ratio $[^{12}\mathrm{CO}/\mathrm{HCN}] \approx 10^3$, then τ_{10}(HCN) is an order of magnitude higher than $\tau_{10}(^{12}\mathrm{CO})$. The resulting T_B(HCN) is sufficiently high to account for a ^{12}CO/HCN line ratio of 9.

Above, we infer a clumpy molecular medium because we chose $\Delta V = 5$ km s^{-1}, yielding small clouds with $r < 1$ pc (see Aalto et al. 1991). We cannot, however, exclude significantly larger ΔV that would indicate a continuous, noncloudy structure—perhaps even a smooth, rotating disk. A third alternative is a molecular interstellar medium (ISM) consisting of dense clumps surrounded by diffuse, noncloudy molecular gas (e.g., Aalto et al. 1994, 1995; Dahmen et al. 1996).

3.2. *The Overlap Region C and NGC 3690*

Molecular line ratio variations are also seen within the overlap region C, albeit smaller than those within IC 694. The weakest ^{13}CO and strongest HCN 1–0 emission, relative to ^{12}CO, are found in C1, the location of the brightest Hα emission in Arp 299 (Gehrz et al. 1983). Continuum emission at 3.4 μm and 10 μm also peaks close to the C1 clump. Thus, C1 appears to be currently the most active star-forming region within C. We suggest that the observed molecular line ratio gradients are the result of a temperature and/or density gradient across the overlap region. The $^{12}\mathrm{CO}/^{13}\mathrm{CO}$ 1–0 line ratio in C1 is considerably lower than in the nucleus of IC 694, perhaps because C1 is an extranuclear starburst.

Unlike ^{12}CO, the ^{13}CO emission peak is not connected with the nucleus of NGC 3690 (B1). The radial excitation gradient is similar, therefore, to that of IC 694, with the highest $^{12}\mathrm{CO}/^{13}\mathrm{CO}$ line ratio in the central region. The nucleus of NGC 3690, with intense associated Hα emission, is a site of starburst activity (Gehrz et al. 1983).

3.3. *Molecular Abundances*

It has been suggested that high $^{12}\mathrm{CO}/^{13}\mathrm{CO}$ intensity ratios in mergers are caused by unusually high isotopic abundance ratios in molecular clouds with optically thick ^{12}CO 1–0 lines. An influx of very low metallicity gas from the outer disk of the galaxies is the proposed cause of such an extreme abundance ratio (e.g., Casoli et al. 1992; Henkel & Mauersberger 1993). Since the $^{12}\mathrm{CO}/^{13}\mathrm{CO}$ intensity ratio is normal in the outskirts of IC 694 and NGC 3690, this scenario is unlikely to be the explanation for Arp 299. Instead, the measured line ratio variations most likely indicate differences in the line excitation and gas properties in different parts of the system.

The observed $^{12}\mathrm{CO}/^{13}\mathrm{CO}$ 1–0 line ratio is, however, a lower limit to the $^{12}\mathrm{CO}/^{13}\mathrm{CO}$ abundance ratio in the emitting region, and for $\tau_{10}(^{12}\mathrm{CO}) \lesssim 1$ this implies an abundance ratio not much greater than 60 in the center of IC 694. This value is typical for GMCs in the Galactic disk, but higher than in the inner region of our Galaxy, where the ratio is $\approx$25 (Langer & Penzias 1990). Perhaps the ISM in the nucleus of IC 694 recently arrived from the disk of the galaxy. In this case, the difference in line ratio between A2 and A1 is solely caused by a dramatic change in mean optical depth of the ^{12}CO line. On the other hand, selective photodissociation of ^{13}CO by a starburst and/or an AGN may change the isotopic abundance ratio. A young nuclear starburst may also produce extra ^{12}C and thus temporarily increase the $^{12}\mathrm{C}/^{13}\mathrm{C}$ abundance ratio (e.g., Henkel & Mauersberger 1993).

4. CONCLUSIONS

The $^{12}\mathrm{CO}/^{13}\mathrm{CO}$ 1–0 line ratio varies dramatically within Arp 299, from 60 $\pm$ 15 at the nucleus of IC 694 to 5–10 in its disk and in the eastern and north interface regions (C3 and D). The ^{13}CO 1–0 brightness, relative to ^{12}CO, is high in quiescent regions of low ^{12}CO surface brightness, and low in starburst regions and galactic nuclei. In contrast, HCN 1–0 is bright in the two galaxy centers and in the active extranuclear star formation region. The ^{12}CO/HCN 1–0 is 9 $\pm$ 1 at the nucleus of IC 694, 14 $\pm$ 3 for NGC 3690, and 11 $\pm$ 3 for the extranuclear starburst region C1. Unusually high $^{12}\mathrm{CO}/^{13}\mathrm{CO}$ line ratios (>20) appear to be associated with extremely compact molecular distributions in the nuclei of merging galaxies (see Aalto et al. 1995).

The large $^{12}\mathrm{CO}/^{13}\mathrm{CO}$ 1–0 intensity ratio at the nucleus of IC 694 can be attributed to low-to-moderate optical depth ($\tau \lesssim 1$) in the ^{12}CO 1–0 line, possibly combined with abundance effects. A medium consisting of dense ($n = 10^4$–10^5 cm^{-3}), warm ($T_k > 50$ K) gas is consistent with the observations.

We thank Peter Bryant for helpful discussions and suggestions. The OVRO mm array is supported in part by NSF grant AST 9314079 and the K. T. and E. L. Norris Foundation. The National Radio Astronomy Observatory is a facility of the National Science Foundation, operated under cooperative agreement by Associated Universities, Inc.

REFERENCES

Aalto, S., Black, J. H., Johansson, L. E. B., & Booth, R. S. 1991, A&A, 249, 323.
Aalto, S., et al. 1994, A&A, 286, 365
Aalto, S., Booth, R. S., Black, J. H., & Johansson. L. E. B. 1995, A&A, 300, 369
Baan, W. A., & Haschick, A. 1990, ApJ, 364, 65
Bryant, P. 1996, Ph.D. thesis, Caltech
Bryant, P., & Scoville, N. Z. 1996, ApJ, 457, 678
Casoli, F., Combes, F., Augarde, R., Figon, P., & Martin, J. M. 1989, A&A, 224, 31
Casoli, F., Dupraz, C., & Combes, F. 1992, A&A, 264, 55
Condon, J. J., Huang, Z.-P., Yin, Q. F., Thuan, & T. X. 1991, ApJ, 378, 65
Dahmen, G., et al. 1996, A&AS, submitted
Gehrz, R. D., Sramek, R. A., & Weedman, D. W. 1983, ApJ, 267, 551
Henkel, C., & Mauersberger, R. 1993, A&A, 274, 730
Langer, W. D., & Penzias, A. A. 1990, ApJ, 357, 477
Rickard, L. J., & Blitz, L. 1985, ApJ, 292, L57
Sargent, A. I., Sanders, D. B., Scoville, N. Z., & Soifer, B. T. 1987, ApJ, 312, L35
Sargent, A. I., & Scoville, N. Z. 1991, ApJ, 366, L1
Scoville, N. Z., Sargent, A. I., Sanders, D. B., & Soifer, B. T. 1991, ApJ, 366, L5
Solomon, P. M., & Sage, L. J. 1988, ApJ, 334, 613
Solomon, P. M., et al. 1992, Downes, D., & Radford, S. J. E. 1992, ApJ, 348, L53
Young, J. S., & Sanders, D. B. 1986, ApJ, 302, 680

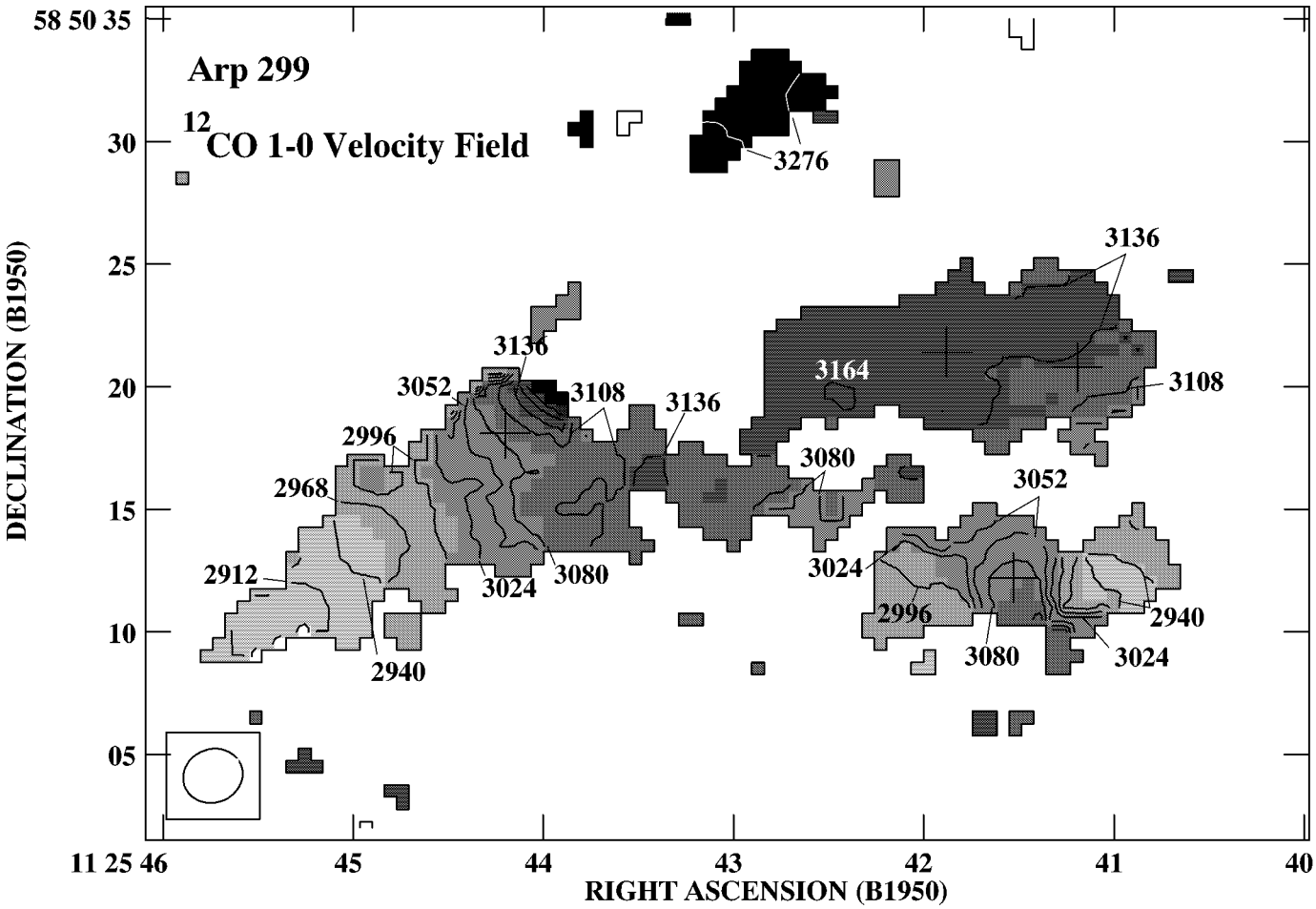

FIG. 2.—The ^{12}CO 1–0 velocity field. The gray-scale ranges from 2800 (*light*) to 3300 (*dark*) km s^{-1}, the contours from 2800 to 3200 km s^{-1}.

ALTO et al. (see 475, L108)